Double-Contrast Upper Gastrointestinal Radiography: A Pattern Approach for Diseases of the Stomach[1]

Stephen E. Rubesin, MD
Marc S. Levine, MD
Igor Laufer, MD

The double-contrast upper gastrointestinal series is a valuable diagnostic test for evaluating structural and functional abnormalities of the stomach. This article will review the normal radiographic anatomy of the stomach. The principles of analyzing double-contrast images will be discussed. A pattern approach for the diagnosis of gastric abnormalities will also be presented, focusing on abnormal mucosal patterns, depressed lesions, protruded lesions, thickened folds, and gastric narrowing.

[1] From the Department of Radiology, Hospital of the University of Pennsylvania, 3400 Spruce St, Philadelphia, PA 19104. Received July 18, 2006; revision requested September 20; revision received October 5; accepted November 2; final version accepted January 2, 2007; final review by M.S.L. June 19. S.E.R. and M.S.L. are paid consultants for E-Z-Em, Westbury, NY. **Address correspondence to** M.S.L. (e-mail: *marc.levine@uphs.upenn.edu*).

This article presents a pattern approach for the diagnosis of diseases of the stomach at double-contrast upper gastrointestinal radiography. After describing the normal appearance of the stomach on double-contrast barium studies and the principles of double-contrast image interpretation, we will consider abnormal surface patterns of the mucosa, depressed lesions (erosions and ulcers), protruded lesions (polyps, submucosal masses, and other tumors), thickened folds, and gastric narrowing.

Essentials

- Protruded lesions (eg, polyps and cancers) on the dependent wall of the stomach may appear as radiolucent filling defects in the barium pool, whereas protruded lesions on the nondependent wall may appear as barium-coated "ring shadows" due to barium coating the edge of these lesions.
- Multiple small, round, uniform nodules in the stomach are usually caused by lymphoid hyperplasia associated with *Helicobacter pylori* gastritis, whereas irregular nonuniform nodules may be caused by low-grade B-cell mucosa-associated lymphoid tissue lymphoma.
- Aspirin and other nonsteroidal antiinflammatory drugs (NSAIDs) are by far the most common cause of erosive gastritis, a condition manifested on double-contrast studies as punctate or slitlike erosions surrounded by radiolucent mounds of edema or, in some patients taking NSAIDs, by linear or serpiginous erosions on or near the greater curvature of the gastric antrum or body.
- *H pylori* gastritis is by far the most common cause of focally or diffusely thickened gastric folds, which can be so large and lobulated (eg, polypoid gastritis) that the radiographic findings resemble those of Menetrier disease or lymphoma.
- On barium studies, scirrhous carcinomas of the stomach may produce a linitis plastica appearance with diffuse narrowing or long- or short-segment narrowing of any portion of the stomach; metastatic breast cancer and lymphoma occasionally may produce a similar radiographic appearance.

Normal Stomach

Gastric Configuration and Rugal Folds

The normal stomach is a J-shaped pouch that lies in the left upper quadrant (Fig 1). The stomach has a fixed configuration created by the greater length of the longitudinal muscle layer on its greater curvature. The lesser curvature of the stomach is suspended from the retroperitoneum by the hepatogastric ligament, a portion of the lesser omentum. The gastrosplenic ligament and gastrocolic ligament (ie, the proximal portion of the greater omentum) are attached to the greater curvature of the stomach. The gastric cardia is attached to the diaphragm by the surrounding phrenoesophageal membrane.

The stomach is arbitrarily divided into five segments: the cardia, fundus, body, antrum, and pylorus. The gastric cardia is characterized on barium studies by three or four stellate folds that radiate to a central point at the gastroesophageal junction, also known as the cardiac "rosette" (Fig 2) (1,2). The gastric fundus is defined as the portion of the stomach craniad to the gastric cardia. The gastric body is defined as the portion of the stomach extending from the gastric cardia to the smooth bend in the mid lesser curvature known as the incisura angularis. The gastric antrum is defined as the portion of the stomach extending from the incisura angularis to the pylorus (a structure created by a muscle sphincter shaped like a figure eight).

Rugal folds are most prominent in the gastric fundus and body, whereas the gastric antrum is often devoid of folds (Fig 1). Gastric rugae are changeable structures composed of mucosa and submucosa (3,4). The rugal folds are relatively straight on the lesser curvature of the stomach but larger and more undulating on the greater curvature. The thickness of the rugal folds varies with the degree of gastric distention (5).

Areae Gastricae

The mucosal surface of the stomach consists of flat polygonal-shaped tufts of mucosa, known as areae gastricae, separated by narrow grooves (6,7). The areae gastricae are recognized on double-contrast studies as a reticular network of barium-coated white lines when barium fills the grooves between these mucosal tufts (Fig 3). Individual mucosal tufts of areae gastricae normally have a diameter of 2–3 mm in the gastric antrum and of 3–5 mm in the gastric body and fundus (Fig 3) (6,8). Areae gastricae are detected on double-contrast studies in nearly 70% of patients and are observed with greater frequency in the elderly (8,9).

Comparison of Histologic Anatomy with Macroscopic Anatomy

A basic understanding of the histologic anatomy of the stomach is helpful for understanding peptic ulcer disease, as well as other gastric abnormalities (5,10). The stomach contains several types of mucosa: cardiac-type mucosa, body/fundic-type mucosa, and antral/pyloric-type mucosa. Gastric foveolae (or pits) are conical depressions in the mucosal surface that communicate with gastric glands (4,10). The glands are long, straight, and tightly packed structures. The foveolae in all parts of the stomach are lined by surface foveolar mucous cells. The cardiac-type mucosa comprises a short (1 cm in length) segment of the gastric mucosa adjacent to the gastroesophageal junction (4). The distinguishing feature of the body-type mucosa is the presence

Published online
10.1148/radiol.2461061245

Radiology 2008; 246:33–48

Abbreviations:
MALT = mucosa-associated lymphoid tissue
NSAID = nonsteroidal antiinflammatory drug

Authors stated no financial relationship to disclose.

of parietal and chief cells in the glands. The parietal cells produce hydrochloric acid and intrinsic factor, and the chief cells produce proteolytic enzymes. No parietal or chief cells are found in antral-type mucosa. The surface foveolar mucous cells line both antral pits and glands.

Body-type mucosa lines the anatomic gastric fundus and the gastric body and extends into the gastric antrum along the greater curvature (4). Antral-type mucosa lines the antrum along the lesser curvature from the pylorus to the incisura angularis, but only lines a small amount of antrum along the greater curvature. Thus, the histologic division of the stomach into body- and antral-type mucosa does not correlate with the anatomic and radiologic division of the stomach into fundus, body, and antrum (5).

The transition zone between body- and antral-type mucosa is a line that extends from the incisura angularis to the distal greater curvature. The transition zone migrates proximally with age, extending progressively higher on the lesser curvature. Peptic ulcers frequently develop on the lesser curvature at the transition zone (Fig 4).

Principles of Image Analysis

Appearance of the Stomach

The radiologist first examines the overall position, shape, and size of the stomach. The gastric fundus abuts the left hemidiaphragm. The cardia has a midline location, abutting the crus of the left hemidiaphragm. The stomach curves to the right across the midline, with the distal gastric antrum and duodenum extending to the right of the spine. There is considerable variation in the size of the stomach, depending on the amount of barium and effervescent agent administered.

Luminal Contour

In the barium pool, the contour is demarcated by a smooth edge of barium (Fig 1). With air contrast, the luminal contour appears as a smooth, continuous barium-coated white line (Fig 1) (11).

Barium Pool

The pool of high-density barium is the tool the radiologist uses to scrub and

Figure 1

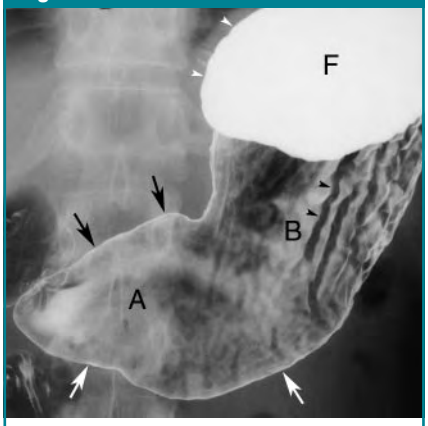

Figure 1: Normal stomach. Double-contrast spot image of stomach with patient supine shows distal gastric body *(B)* and antrum *(A)*. Greater curvature (white arrows) and lesser curvature (black arrows) are coated by barium. Rugal fold on posterior wall of gastric body is depicted as tubular, slightly undulating, radiolucent filling defect (black arrowheads) in shallow barium pool. Dense barium pool outlines contour (white arrowheads) of gastric fundus *(F)*. Mucosal surface and folds in fundus are obscured by barium pool, and antrum is devoid of rugal folds.

Figure 2

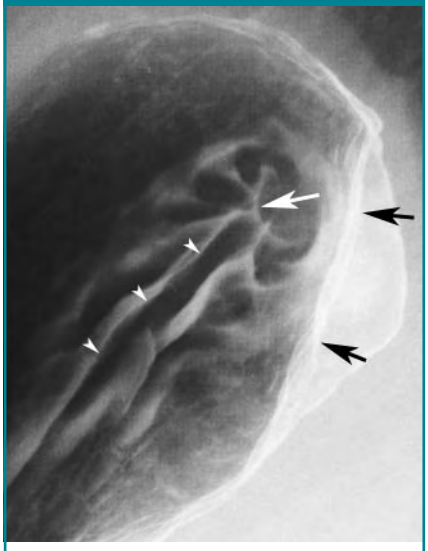

Figure 2: Double-contrast spot image of gastric fundus with patient in right-side-down position shows normal gastric cardia with smooth folds radiating to central point (white arrow) at closed gastroesophageal junction, also known as cardiac rosette. Long, straight fold (arrowheads) extends inferiorly from cardia along lesser curvature. Black arrows denote normal extrinsic impression by adjacent spleen.

Figure 3

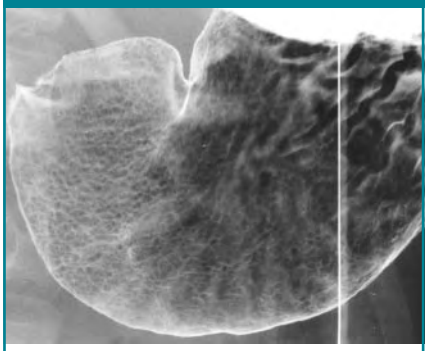

Figure 3: Double-contrast spot image of stomach with patient in left posterior oblique position shows normal areae gastricae pattern in antrum as 2–3-mm polygonally shaped radiolucent tufts of mucosa outlined by barium in grooves. Areae gastricae are slightly larger in distal gastric body than in antrum.

Figure 4

Figure 4: Double-contrast spot image of stomach with patient in supine position shows benign lesser curvature gastric ulcer *(U)* as smooth, ovoid collection of barium extending outside expected luminal contour of gastric body. Smooth folds are seen radiating to edge of ulcer crater.

coat the mucosal surface (12–15). Some lesions are best shown in the barium pool, whereas others are obscured by even a small pool of high-density barium. Protruded lesions on the dependent wall usually appear as radiolucent filling defects in the barium pool (Fig 5) (16), whereas protruded lesions on the nondependent wall appear as barium-coated "ring shadows" due to barium coating the edge of these lesions (Fig 5). When filled with barium, depressed lesions appear as barium collections on the dependent wall (Fig 4). When barium spills out of depressed lesions on the dependent wall, they may appear as ring shadows.

Figure 5

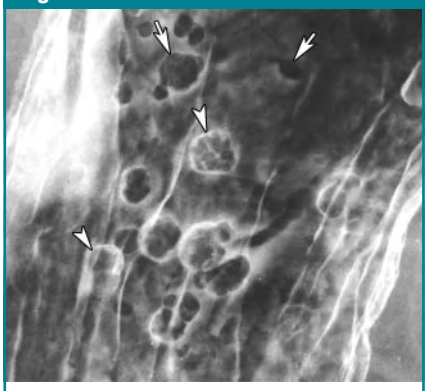

Figure 5: Double-contrast spot image of gastric body with patient in supine right posterior oblique position shows multiple hyperplastic polyps on dependent, or posterior, wall as small (< 1 cm in size), round or ovoid, finely lobulated radiolucent filling defects in barium pool (arrows). In contrast, polyps on nondependent, or anterior, wall are coated by barium and appear as white lines (arrowheads). Barium is seen to fill interstices between lobules of some polyps.

Figure 6

Figure 6: Double-contrast spot image of antrum with patient in supine position shows gastric striae as transient finding due to barium filling delicate transverse grooves between thin radiolucent folds traversing circumference of slightly collapsed gastric antrum.

En Face Mucosal Detail

When viewed en face, the mucosal surface either has a smooth appearance (Fig 1) or is manifested as a reticular network of barium-filled grooves between the areae gastricae (Fig 3). Disruption of the normal areae gastricae pattern or the smooth mucosal surface of the stomach by barium-coated lines is abnormal (Fig 5).

Pattern Approach for Double-Contrast Diagnosis

Abnormal Mucosal Patterns

Striations.—Thin, barium-coated striations perpendicular to the longitudinal axis of the gastric antrum, also known as gastric "striae," are sometimes seen as a transient finding when the antrum is slightly collapsed (Fig 6) (17). These striae are a sign of chronic antral gastritis (16).

Conspicuous or enlarged areae gastricae.—Visualization of the areae gastricae in the stomach depends on the thickness of barium in the grooves between the mucosal tufts in relation to the thickness of barium overlying the tufts (8,9). Thus, an increase in the height of the mucosal tufts or thinning of the mucous gel layer in the stomach may cause the areae gastricae to become more visible or conspicuous. When viewed in profile, barium in the grooves between areae gastricae may be manifested as tiny spike-like outpouchings, producing subtle spiculation of the luminal contour that should not be mistaken for erosions. In addition, the areae gastricae may be enlarged by conditions that increase the size of the mucosal tufts beyond their normal diameter of 2–3 mm in the antrum and of 3–5 mm in the body and fundus. Enlarged areae gastricae have been reported in about 50% of patients with *Helicobacter pylori* gastritis (Fig 7) (18). In contrast, small or even absent areae gastricae have been reported in patients with severe atrophic gastritis and pernicious anemia (19).

Figure 7

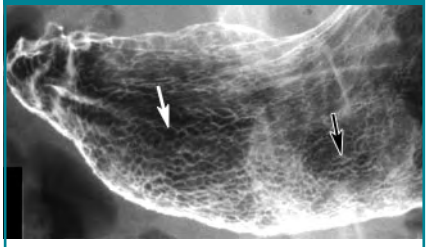

Figure 7: Double-contrast spot image of stomach with patient in supine position shows enlarged areae gastricae in patient with *H pylori* gastritis. Areae gastricae in antrum (white arrow) are larger than those in distal gastric body (black arrow).

H pylori is a curved or spiral-shaped, gram-negative bacillus (20–22) that infects the stomach in more than 50% of Americans over 50 years of age and in nearly 100% of Japanese adults (23,24). *H pylori* most frequently involves the gastric antrum (25). *H pylori* gastritis can be documented in almost all patients with duodenal ulcers and in about 80% of patients with gastric ulcers (26). The mechanism by which *H pylori* causes ulceration is not fully understood. *H pylori* gastritis is also a major causative factor in the development of both gastric carcinoma (27,28) and gastric lymphoma (29,30).

Uniform nodules.—Innumerable small (1–2 mm in size), round, uniform nodules disrupting the normal polygonal areae gastricae pattern are usually caused by lymphoid hyperplasia of the stomach resulting from chronic *H pylori* gastritis (Fig 8) (31–33). At birth, no lymphoid tissue is present in the stomach. When *H pylori* infects the stomach, the organism colonizes the mucous layer and attaches to the membranes of the surface epithelial cells, resulting in the development of chronic gastritis

(22). Repeated infections may eventually lead to lymphocytic infiltration of the stomach, followed by the formation of lymphoid aggregates and even true lymphoid follicles (34). Thus, when lymphoid hyperplasia is detected on double-contrast barium studies, these patients are almost always found to have chronic *H pylori* gastritis (33).

Nonuniform nodules.—Irregular nodules disrupting the smooth mucosal surface or the polygonal areae gastricae pattern of the stomach may be caused by inflammation, metaplasia (alteration of one form of epithelium to another), or malignant tumor. The nodules are nonuniform in size and shape and have a patchy or diffuse distribution, involving a focal or large surface area of the stomach on barium studies. Nonuniform mucosal nodularity is a worrisome radiographic finding for gastric mucosa-associated lymphoid tissue (MALT) lymphoma (Fig 9) or, rarely, superficial spreading carcinoma (Fig 10) (35).

Gastric lymphomas usually arise from preexisting MALT in the stomach associated with chronic *H pylori* gastritis. A lymphoid response to chronic infection by *H pylori* has been postulated as the precursor milieu for the development of low-grade B-cell gastric MALT lymphomas (36). These tumors are sometimes recognized on double-contrast studies by the presence of innumerable poorly defined, confluent mucosal nodules of varying size (Fig 9) (35). In such cases, endoscopic biopsy specimens are required to rule out gastric MALT lymphoma.

Because of mass screening of the adult population in Japan, early gastric cancers (EGCs) constitute as many as 25%–46% of all gastric cancers detected in that country (37,38). In contrast, EGCs constitute a much smaller percentage of gastric cancers detected in the West, because endoscopy and barium studies are performed predominantly in symptomatic patients who already have advanced lesions (39–41). In the Japanese classification system for EGC, polypoid EGCs that protrude more than 5 mm into the lumen are type I lesions; flat EGCs that appear as plaques, nodules, or tiny ulcers are type IIa (elevated), IIb (flat), or IIc (depressed) lesions (Fig 10); and ulcerated EGCs that are more than 5 mm in depth are type III lesions (42).

Figure 8

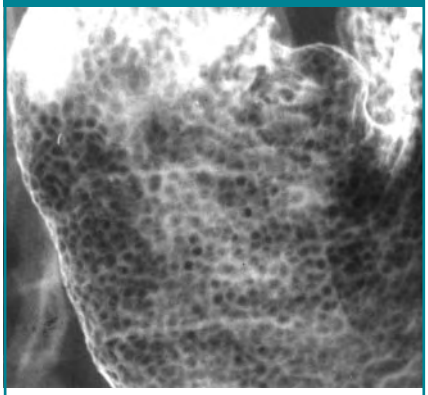

Figure 8: Double-contrast spot image of gastric antrum with patient in left posterior oblique position shows lymphoid hyperplasia with innumerable round, uniform, 1–2-mm nodules carpeting mucosa and replacing normal polygonal areae gastricae pattern. This patient had chronic *H pylori* gastritis.

Figure 9

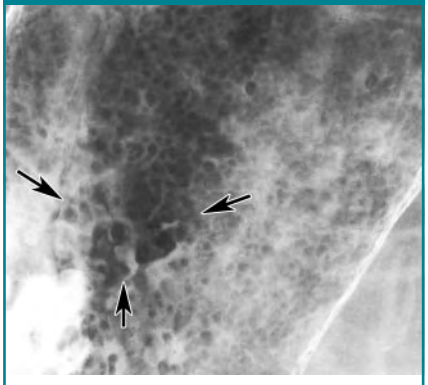

Figure 9: Double-contrast spot image of gastric body with patient in right posterior oblique position shows nonuniform nodules disrupting normal surface pattern. Nodules (arrows) appear as round or lobulated, confluent protrusions varying from 3–6-mm in size. Endoscopic biopsy specimens revealed low-grade, B-cell, gastric MALT lymphoma in patient with chronic *H pylori* gastritis.

Figure 10

Figure 10: Double-contrast spot image of gastric fundus with patient in semiupright position shows superficial gastric carcinoma as focal area of slightly elevated, irregular radiolucent nodules (arrows) in shallow barium pool. Clubbed, irregular folds (arrowheads) are seen radiating toward central area of mucosal nodularity.

Depressed Lesions

Erosions.—An erosion is a focal area of mucosal necrosis confined to the epithelium or lamina propria without extending through the muscularis mucosae into the submucosa (5). In contrast, a true ulcer niche or crater extends through the muscularis mucosae into the deeper layers of the gastric wall (4). The actual histologic depth of an ulcer cannot be determined on barium studies. Instead, the radiographic size and depth are used to distinguish an erosion from an ulcer. When viewed in profile, a depressed lesion greater than several millimeters in depth is arbitrarily called an ulcer.

Erosions are manifested on double-contrast studies as tiny, 1–2 mm in depth collections of barium, usually in the gastric antrum. Erosions may be punctate, round, linear, or stellate in configuration and are often surrounded by radiolucent halos of edematous mucosa (Fig 11) (43). Erosions are frequently seen to reside on the crests of enlarged scalloped antral folds (44), particularly when the patient is slowly turned from side to side, so a shallow pool of barium flows over the dependent surface of the stomach (45). Erosions are defined as complete or varioliform if surrounded by a radiolucent halo of edema and as incomplete if there is no surrounding edematous mound. Incomplete erosions are much less common,

appearing as punctate or linear collections of barium that may be difficult to differentiate from barium trapped between areae gastricae or alongside rugal folds.

Aspirin and other nonsteroidal antiinflammatory drugs (NSAIDs) are by far the most common cause of gastric erosions (46). NSAID exposure causes breakdown of the mucosal barrier and mucosal hypoxia, resulting in focal areas of epithelial necrosis with hemorrhage, edema, and vascular dilatation in the lamina propria (47). Because often there is relatively little inflammatory response, the term *NSAID gastropathy* rather than *NSAID gastritis* is favored by some authors (10,48). NSAID-induced erosive gastritis is typically manifested as multiple varioliform erosions in the antrum or antrum and body of the stomach (18). Less frequently, these patients may have incomplete erosions that appear as linear or serpiginous barium collections (Fig 12), many of which are located on or near the greater curvature of the gastric body secondary to the effect of gravity (49).

Figure 11

Figure 11: Double-contrast spot image of distal gastric antrum with patient in left posterior oblique position shows NSAID-induced erosive antral gastritis. Multiple varioliform erosions are seen as punctate (small white arrow) and linear (large white arrow) collections of barium surrounded by radiolucent mounds of edema (black arrows). This patient was taking aspirin.

Figure 12

Figure 12: Double-contrast spot image of gastric antrum with patient in left posterior oblique position shows NSAID-induced linear and serpiginous erosions (arrows). This patient was taking aspirin. Surgical clips in right upper quadrant are from prior cholecystectomy.

Figure 13

Figure 13: Double-contrast spot image of gastric body with patient in left posterior oblique position shows gastric ulcer *(U)* as smooth, ovoid collection of barium on posterior wall. Smooth, straight folds radiate directly to edge of ulcer crater. These are typical findings of a benign gastric ulcer.

Figure 14

Figure 14: Double-contrast spot image of gastric body with patient in supine position shows incompletely filled ulcer on dependent, or posterior, wall as hemispheric ring shadow with two crescent-shaped barium-coated lines (arrows) coating various portions of inferior rim of ulcer. Smooth, straight folds radiate almost to edge of ulcer crater. The findings are characteristic of a benign gastric ulcer with retraction of adjacent gastric wall.

Other causes of gastric erosions include alcohol, viral infections, Crohn disease, hemorrhagic gastropathy, and iatrogenic trauma (4,50–55). Surprisingly, erosions are infrequently seen in patients with *H pylori* gastritis (18).

Ulcers.—An ulcer is a focal area of mucosal disruption that penetrates through the muscularis mucosae into the deeper layers of the gastric wall. When viewed en face, most benign gastric ulcers on the dependent wall are manifested on double-contrast studies as a smooth round or ovoid collection of barium filling the ulcer crater (Fig 13). Some shallow ulcers on the dependent wall and ulcers on the nondependent wall may be manifested as a circular or hemispheric ring due to barium coating the rim of the unfilled ulcer crater (Fig 14) (56). Most ulcers are round or ovoid, but some may have a linear, serpentine, rectangular, flame-shaped, or rod-shaped configuration (56–58).

When viewed in profile, benign gastric ulcers may be recognized by a focal barium collection or barium-coated line extending outside the expected luminal contour (Fig 4) (11,59–61). Some ulcers have a smooth radiolucent rim of variable thickness directly adjacent to the ulcer crater, representing a collar of edema and inflammation, whereas others have a thin radiolucent line (also known as a Hampton line) traversing the base of the crater due to undermining of the submucosa (59). The presence of a Hampton line is diagnostic of a benign gastric ulcer. Chronic inflamma-

tion and scarring may cause retraction of the adjacent gastric wall with the development of smooth, straight folds that radiate directly to the edge of the ulcer crater (Figs 13, 14).

Although giant gastric ulcers are at greater risk for bleeding and perforation (62), the size of the ulcer crater is not a useful criterion for differentiating benign and malignant gastric ulcers. Most benign gastric ulcers are located on the lesser curvature or posterior wall of the stomach at or near the transition zone between body- and antral-type mucosa (Fig 4). Some benign ulcers may be located on the greater curvature (almost all of these greater curvature ulcers are caused by the use of aspirin or other NSAIDs) (14,63) or within hiatal hernias, where the stomach traverses the diaphragm (64). Thus, ulcer location also is not a useful criterion for differentiating benign and malignant gastric ulcers. Radiologists therefore should ignore the size and location of ulcers when assessing the risk of malignancy; instead, they should focus on the morphologic features of these lesions.

In general, malignant gastric ulcers produce radiographic findings diametrically opposed to those of benign ulcers. With malignant ulcers, the ulcer crater represents a focal area of necrosis and excavation within a malignant tumor, usually gastric carcinoma or lymphoma. The surface of the ulcer and of the surrounding mucosa is therefore composed of nodules, irregular elevations, or irregular depressions of varying size within the tumor (Fig 15) (42). The folds adjoining a malignant ulcer may have a coarse, lobulated, clubbed, or penciled shape due to infiltration of the folds by the tumor (Fig 10) (42).

Radiologists can often differentiate benign and malignant gastric ulcers on the basis of the radiographic findings (Fig 16). If an ulcer has a smooth surface with smooth, straight folds radiating to the ulcer margin and no surrounding mass effect or mucosal nodularity (Figs 4, 13, 14), it fulfills the radiographic criteria for a benign gastric ulcer. About two-thirds of all gastric ulcers diagnosed on double-contrast barium studies have an unequivocally benign radiographic appearance; virtually all of these unequivocally benign ulcers are ultimately proved to be benign (56,65).

Figure 15

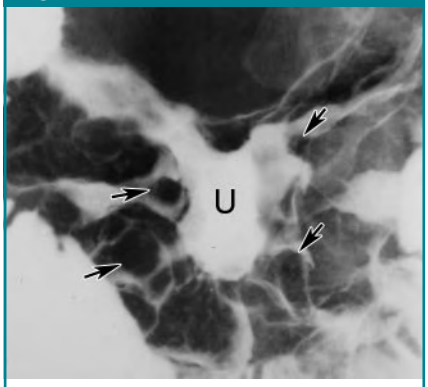

Figure 15: Double-contrast spot image of gastric body with patient in supine position shows malignant gastric ulcer due to lymphoma. Large lobules of tumor (arrows) surround irregular central ulcer *(U)* filled with barium, although barium pool is too dense to clearly delineate margins of ulcer.

In contrast, if an ulcer is associated with nodularity of the adjacent mucosa, mass effect, or radiating folds that are coarse, lobulated, or irregular (Figs 10, 15), it fulfills the radiographic criteria for a malignant gastric ulcer, and endoscopy should be performed for a definitive diagnosis. Less than 5% of ulcers have an unequivocally malignant radiographic appearance; almost all of these malignant-appearing ulcers are ultimately proved to be malignant.

Finally, one-fourth to one-third of gastric ulcers have an equivocal or indeterminate appearance that does not allow the radiologist to establish a confident diagnosis of benignancy or malignancy. An ulcer is classified as equivocal or indeterminate if there are coarse areae gastricae or moderate nodularity of the mucosa abutting the ulcer (Fig 17), a nodular ulcer collar, or mildly irregular folds radiating to the ulcer's edge. In such cases, endoscopy and biopsy are needed to rule out malignant tumor. Nevertheless, the majority of equivocal or indeterminate ulcers are ultimately proved to be benign.

Some benign NSAID-induced greater

Figure 16

Benign

Smooth, round/ovoid barium collection/ring shadow
Hampton's line or smooth ulcer collar
Smooth, straight folds radiating to ulcer's edge
Projects outside expected luminal contour

Malignant

Irregular-shaped, abnormally surfaced ulcer
Mucosal nodularity at ulcer's edge
Lobulated, enlarged, club-shaped, or pencil point-shaped folds
Projects into mass (either inside or outside expected luminal contour)

Figure 16: List of radiographic features distinguishing benign and malignant gastric ulcers.

Figure 17

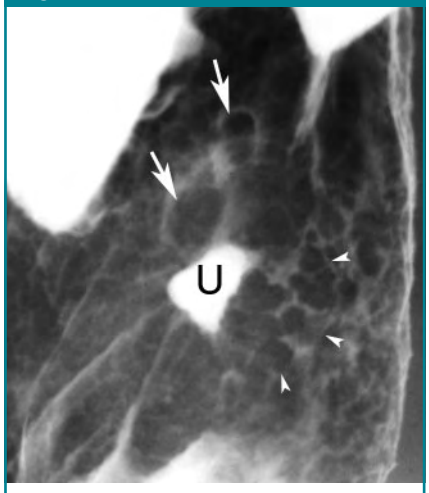

Figure 17: Double-contrast spot image of gastric body with patient in right posterior oblique position shows ulcer *(U)* on posterior wall filling with barium. Small radiolucent nodules (arrowheads) are seen lateral to ulcer and larger nodules (arrows) are seen just superior to ulcer. This nodularity could be secondary to edema, inflammation, metaplasia, dysplasia, or tumor; findings in this case do not meet radiographic criteria for a benign gastric ulcer, and lesion should be classified as equivocal. Nevertheless, benign gastric ulcer was confirmed at endoscopy and follow-up. Gastric metaplasia was found at the edge of the ulcer on endoscopic biopsy specimens.

curvature ulcers may have an indeterminate appearance due to extensive surrounding mass effect and an apparent intraluminal location because of spasm and inflammatory retraction of the adjacent greater curvature (66). Despite a history of NSAID use, these greater curvature ulcers therefore may require endoscopy to rule out an ulcerated gastric carcinoma. Eventually, large NSAID-induced greater curvature ulcers may penetrate inferiorly via the gastrocolic ligament into the superior border of the transverse colon, producing a gastrocolic fistula (67).

Diverticula.—Diverticula are uncommonly found in the stomach. The majority arise from the posterior wall of the gastric fundus (68), presumably because of a gap in the muscular layers of the gastric wall in this location. Fundal diverticula are smoothly contoured, broad-mouthed outpouchings, ranging from 1 to 10 cm in size (Fig 18). Rugal folds are not seen within the diverticula. These diverticula can be distinguished from ulcers by their smooth contour, broad or shallow necks, and lack of folds radiating to their margins.

A variant of a gastric diverticulum may rarely be found on the greater curvature of the distal antrum, also known as a partial antral diverticulum (69). These tiny sacs are thought to represent the sequela of healed peptic ulcers. Partial antral diverticula are differentiated from true ulcers by their variable size and shape at fluoroscopy and the absence of associated inflammatory changes.

Figure 18

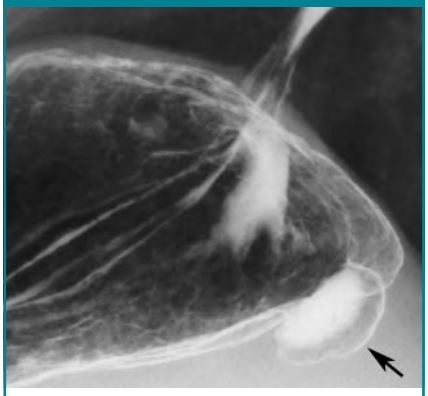

Figure 18: Double-contrast spot image with patient in right decubitus position shows gastric diverticulum as smooth barium-coated outpouching (arrow) extending from posterior wall of fundus. A small amount of barium is present in lumen of diverticulum.

Figure 19

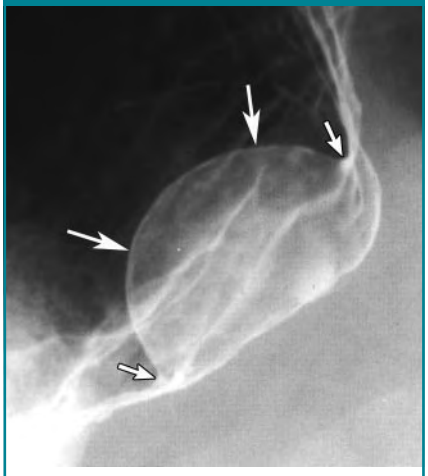

Figure 19: Double-contrast spot image of fundus and upper body of stomach with patient in semiupright position shows large submucosal mass as smooth-surfaced hemispheric lesion (large arrows) forming right angles (small arrows) with adjacent luminal contour. Surgery revealed benign gastrointestinal stromal tumor.

Figure 20

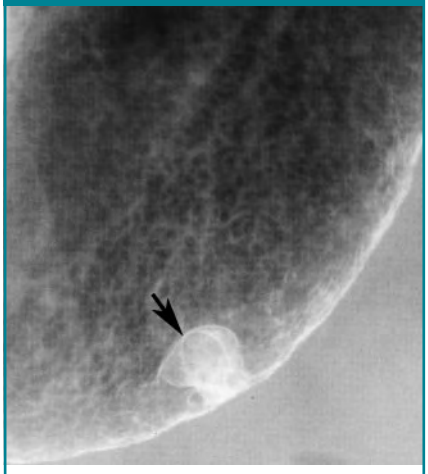

Figure 20: Double-contrast spot image of gastric body with patient in supine position shows 1-cm in size, sessile, slightly lobulated polyp on greater curvature as area of increased radiopacity coated by barium (arrow). Although radiographic findings are worrisome for an adenomatous polyp or even a small polypoid carcinoma, this lesion was found to be a large hyperplastic polyp on endoscopic biopsy specimens.

Protruded Lesions

Polyps.—A polyp is a small protrusion from the mucosal surface, either sessile or pedunculated. The term *polyp* does not imply an adenomatous histology. In fact, a wide variety of benign and malignant polypoid lesions may occur in the stomach. If polyps arise from the mucosa, they may have a smooth, nodular, or lobulated surface on double-contrast studies, and when viewed in profile, form acute angles with the adjacent gastric wall (Fig 5) (70). In contrast, lesions arising from the submucosa or muscularis propria usually have a very smooth surface and, when viewed in profile, form right angles or slightly obtuse angles with the adjacent gastric wall (Fig 19). Although large lesions that have a smooth surface are usually submucosal in origin, it is often difficult to determine whether protruded lesions less than 1–1.5 cm in diameter are mucosal or submucosal in origin, as small polyps originating in the mucosa may also have a smooth surface.

Hyperplastic polyps are nonneoplastic proliferations of surface foveolar cells, consisting of elongated, distorted pits and numerous branching glands (4). These polyps are typically smooth or finely lobulated sessile lesions less than 1 cm in size (Fig 5). Occasionally, however, atypical hyperplastic polyps may be larger than 1 cm in diameter, pedunculated, and have a coarsely lobulated surface (Fig 20) (71–73). At least one-third of patients with hyperplastic polyps have multiple polyps, usually in the gastric body and fundus (Fig 5) (4). Although hyperplastic polyps have no malignant potential, they usually arise in the setting of chronic gastritis, the same milieu that results in gastric metaplasia and dysplasia. As a result, gastric adenomas and carcinomas have been reported to occur with increased frequency in patients with hyperplastic polyps (4).

Fundic gland polyps, the second most common gastric polyps, are proliferations of the deep epithelial compartment of body-type mucosa (4). These polyps consist of cystically dilated pits and glands lined by parietal and chief cells. Fundic gland polyps are found both sporadically and in patients with familial adenomatous polyposis syndrome. These polyps typically appear on double-contrast studies as smooth-surfaced, sessile protrusions less than 1 cm in size. Fundic gland polyps are usually located in the fundus and upper body of the stomach and are often multiple (74). In patients with familial adenomatous polyposis syndrome, hundreds of small (< 5 mm in size) fundic gland polyps may be found.

Adenomatous polyps of the stomach are a relatively uncommon macroscopic form of gastric dysplasia. Adenomas are classified as tubular, tubulovillous, or villous on the basis of their underlying architecture. Gastric adenomas may progress to gastric carcinoma by means of a polypoid adenoma to carcinoma sequence similar to that found in the colon. In situ carcinoma or invasive carcinoma is found in at least 50% of adenomatous polyps larger than 2 cm in size (75). Most gastric dysplasias, however, are relatively flat macroscopically. In fact, most gastric carcinomas arise from flat or slightly elevated or depressed areas of dysplasia, not polypoid adenomas (4).

In symptomatic patients, gastric adenomas detected on double-contrast studies are usually larger than 1 cm in size (75). These adenomas can be sessile, lobulated, or pedunculated lesions (Fig 21). Although most hyperplastic polyps are smaller than 1 cm and most adenomas are larger than 1 cm, it is not always possible to distinguish a hyperplastic polyp from an adenomatous polyp on barium studies. If a polyp is 1 cm or larger in size and has a finely nodular or lobulated surface, endoscopy and biopsy therefore should be performed to exclude the possibility of an adenoma. Conversely, multiple rounded polyps 5 mm or smaller in size are almost always hyperplastic, so that endoscopy and biopsy are not warranted in these patients. Atypical hyperplastic polyps that are unusually large or lobulated (Fig 20) are indistinguishable from adenomatous polyps or even polypoid carcinomas (71–73).

Retention polyps (juvenile polyps) may occur as solitary lesions or as multiple lesions in Cronkite-Canada syndrome (76). Xanthelasmas, isolated hamartomatous polyps, and inflammatory fibroid polyps are other benign polyps occasionally encountered in the stomach. A focal cluster of polyps may also be seen in the gastric antrum or body in patients with small carcinoid tumors.

Masses.—For gastric masses larger than 2 cm in size, barium studies are extremely helpful for determining whether the lesions arise from the mucosa, submucosa, or muscularis propria, or whether they are extrinsic to the stomach. This differentiation enables the radiologist to suggest a specific diagnosis or differential diagnosis. In general, a mass originating in the mucosa has a nodular or lobulated surface, appearing en face on double-contrast studies as a filling defect in the barium pool or as an area of abnormal barium-coated lines, depending on whether it is on the dependent or nondependent walls (Fig 22) (11). Not infrequently, irregular collections of barium are trapped in the interstices of the tumor (Fig 21) or in areas of ulceration. Barium thus outlines multiple round or ovoid nodules within the interstices of the lesion. For example, a polypoid carcinoma may be manifested as a lobulated or fungating mass within the expected luminal contour (Fig 22).

In contrast, a submucosal mass may appear en face on double-contrast studies as a round or ovoid, well-circumscribed, smooth or slightly lobulated area of increased radiopacity. When viewed in profile, a submucosal mass may be manifested as a hemispheric intraluminal projection that has a smooth surface and forms right angles or slightly oblique angles with the adjacent gastric wall (Figs 19, 23). Central ulceration occurs in about 50% of submucosal masses due to central ischemia and necrosis of the tumor or pressure necrosis of the overlying epithelium (Fig 23) (4). An ulcerated submucosal mass viewed en face produces a characteristic "target" or "bull's-eye" lesion, with a central ulcer surrounded by a smooth, well-defined mass (Fig 24). Gastrointestinal stromal tumors are by far the most

Figure 21

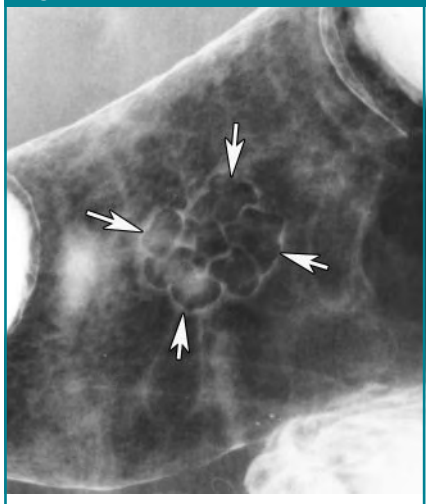

Figure 21: Double-contrast spot image of gastric body with patient in supine position shows barium outlining outer contour and interstices of a 3-cm sessile, multilobulated lesion (arrows). Surgery revealed tubulovillous adenoma. (Reprinted, with permission, from reference 15.)

Figure 22

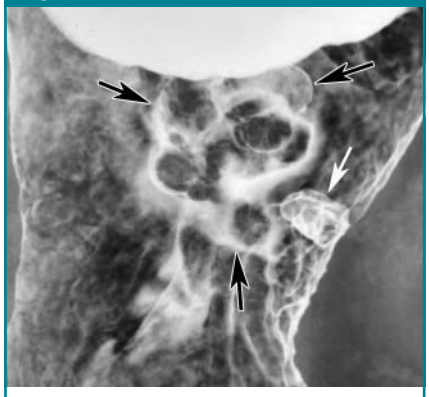

Figure 22: Double-contrast spot image of upper gastric body with patient in supine position shows multilobulated polypoid mass as confluent, lobulated radiolucent filling defects (black arrows) in barium pool with separate portion of lesion outlined in white on greater curvature (white arrow). Surgery revealed polypoid adenocarcinoma.

common solitary submucosal masses in the stomach (77). Lymphoma and solitary metastases are other frequent submucosal tumors. Lipoma is a submucosal lesion that may change in size and shape at fluoroscopy (78) and has fat attenuation at computed tomography (79,80). Granular cell tumors usually appear as one or more small submucosal lesions. Most other mesenchymal tumors (eg, neurofibromas) are indistinguishable from gastrointestinal stromal tumors.

Ectopic pancreatic rest (ie, myoepithelial hamartoma) is an uncommon submucosal lesion composed of varying amounts of pancreatic tissue (including ducts, acini, and islet cells), hypertrophic smooth muscle fibers, and glandular structures resembling Brunner glands (81,82). These lesions may be complicated by pancreatitis, cysts, islet cell tumors, and even pancreatic carcinoma (4). Ectopic pancreatic rests usually appear on barium studies as small (1–2 cm), solitary, centrally umbilicated submucosal masses, most often on the greater curvature of the distal gastric antrum within 1–6 cm from the pylorus, but can occasionally be located elsewhere in the stomach (Fig 25) (83).

Figure 23

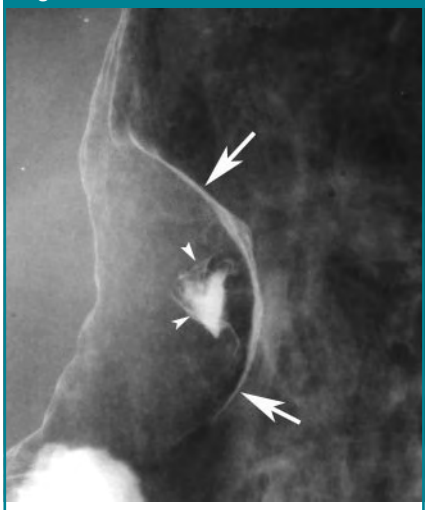

Figure 23: Double-contrast spot image of gastric body with patient in supine position shows 4-cm smooth-surfaced submucosal mass outlined in white by barium (arrows). Note central triangular-shaped ulcer (arrowheads) in mass. Surgery and clinical follow-up revealed a malignant gastrointestinal stromal tumor.

Figure 24

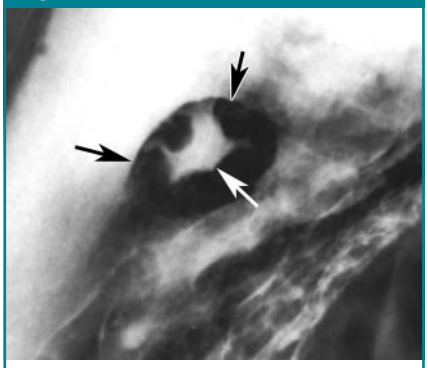

Figure 24: Double-contrast spot image of gastric body with patient in right posterior oblique position shows bull's-eye or target lesion in stomach as a 2-cm ovoid, smooth-surfaced, submucosal mass (black arrows) in barium pool containing stellate central ulcer (white arrow). This patient had breast cancer with hematogenous metastasis to the stomach.

Figure 25

Figure 25: Double-contrast spot image of gastric antrum with patient in left posterior oblique position shows smooth, 1-cm ovoid, radiolucent filling defect (arrow) in barium pool with shallow central umbilication containing trace amount of barium (arrowhead). Endoscopic biopsy specimens revealed an ectopic pancreatic rest (myoepithelial hamartoma). Ectopic pancreatic rests are usually located on greater curvature of distal antrum, but this lesion was on posterior wall.

An extrinsic mass that indents but does not infiltrate the gastric serosa is manifested as a smooth, broad-based inbowing of the gastric wall (Fig 26). In contrast, an extrinsic inflammatory or neoplastic mass that involves the serosa of the stomach may cause tethering of the gastric wall toward the extrinsic process, resulting in spiculation of the luminal contour. For example, omental metastases invading the greater curvature of the stomach through the gastrocolic ligament may cause spiculation and tethering of the greater curvature (84). Extrinsic inflammatory or neoplastic processes that involve the gastric wall or occlude gastric lymphatic or venous channels may also result in enlarged gastric folds. For example, pancreatitis secondarily involving the stomach may be manifested as thickened folds on the posterior gastric wall.

The precise location of mass lesions in the stomach may help suggest the diagnosis in a small percentage of cases. As previously discussed, a submucosal lesion on the greater curvature of the distal gastric antrum should suggest an ectopic pancreatic rest, whereas a submucosal defect extending from the lesser curvature of the distal antrum to the pylorus should suggest a hypertrophied antral-pyloric fold. In contrast, a smooth, undulating submucosal lesion on the medial aspect of the fundus near the gastric cardia should suggest a conglomerate mass of gastric varices (85).

Multiplicity of lesions is another radiographic feature that may be helpful in suggesting a specific diagnosis or differential diagnosis. Numerous small (< 1 cm in size), smooth or finely lobulated, sessile protrusions are almost always hyperplastic polyps (Fig 5) or, if confined to the gastric body or fundus, fundic gland polyps. A cluster of polyps elsewhere in the stomach in patients with chronic *H pylori* gastritis may represent gastric carcinoid tumors due to end-stage neuroendocrine hyperplasia associated with hypogastrinemia (5,10). Multiple large (> 1 cm in size) polypoid lesions may represent adenomatous polyps, atypical hyperplastic polyps, Peutz-Jeghers hamartomas, or even synchronous polypoid carcinomas.

Finally, multiple submucosal masses or centrally ulcerated bull's-eye lesions may represent hematogenous metastases (such as metastatic melanoma), disseminated lymphoma, and, in patients with acquired immunodeficiency syndrome, Kaposi sarcoma.

Thickened Folds

Normal rugal folds are thicker in the proximal stomach, have a smooth contour in profile, and taper distally (5). Folds also are larger and more undulating on the greater curvature than on the lesser curvature. Rugal folds become straight and thinner with increasing gastric distention and can even disappear when the stomach is fully distended, particularly in the gastric antrum. Because of these normal variations in fold size, there are no reliable criteria for enlarged folds in the stomach. However, rugal folds are much more likely to be abnormal when they have an irregular, lobulated, or scalloped contour or when they are enlarged or have an angled or transverse orientation in a well-distended gastric antrum. Folds that are larger on the lesser curvature than on the greater curvature are also considered to be abnormal.

Because rugal folds are composed of mucosa and submucosa, any process that infiltrates these layers of the gastric wall can increase the size of the folds. Enlarged folds may be caused by inflammatory processes such as *H pylori* gastritis (86–89), hyperplastic processes such as Zollinger-Ellison syndrome (90) and Menetrier disease (91), or malignant tumors such as lymphoma and submucosally infiltrating adenocarcinoma. Endoscopic biopsy specimens may be required to differentiate these various causes of enlarged folds, particularly when the folds are markedly thickened and irregular.

Antral gastritis (whether or not it is associated with *H pylori*) is usually manifested on barium studies as thickened, scalloped folds that have a longitudinal or transverse orientation. Antral gastritis may lead to the development of a hypertrophied antral-pyloric fold, seen as a smooth submucosal defect extending from the lesser curvature of the distal antrum to the pylorus or even through the pylorus into the medial fornix of the base of the duodenal bulb (Fig 27) (92). In most patients, a hypertrophied antral-pyloric fold can be differentiated from a neoplastic lesion by its characteristic appearance and location (93). Another clue to the presence of a hypertrophied antral-pyloric fold is its variable size and shape at fluoroscopy, with palpation and peristalsis. Occasionally, however, a hypertrophied fold may be unusually large or lobulated, so it can be mistaken for a polypoid or plaquelike tumor (93).

H pylori gastritis is by far the most common cause of focally or diffusely thickened folds in the stomach. Abnormal folds are found in about 75% of patients with *H pylori* gastritis (89). Fold enlargement in *H pylori* gastritis most commonly involves the gastric antrum and body but may involve the entire stomach or may even be confined to the gastric fundus. Most patients with *H pylori* gastritis have mildly to moderately thickened gastric folds without substantial fold irregularity (Fig 28), so that the radiographic findings are not worrisome for Menetrier disease or lymphoma. However, some patients with *H pylori* gastritis have such enlarged, lobulated folds (ie, polypoid gastritis) that the radiographic findings erroneously suggest a malignant process. Other patients with *H pylori* gastritis may have focally thickened polypoid folds confined to the gastric antrum or body that are mistaken radiographically for a polypoid or infiltrating neoplasm (88). Nevertheless, radiologists cannot assume that all cases of enlarged folds are caused by this ubiquitous pathogen. If the folds are markedly enlarged, lobulated, or irregular (particularly if they have a focal or segmental distribution), endoscopic biopsy specimens should be obtained to exclude a malignant tumor.

In Menetrier disease, there is marked hyperplasia of surface foveolar mucous cells (4,10), resulting in a marked increase in the height of the foveolae and partial atrophy of the glands, with a corresponding loss of vol-

Figure 26

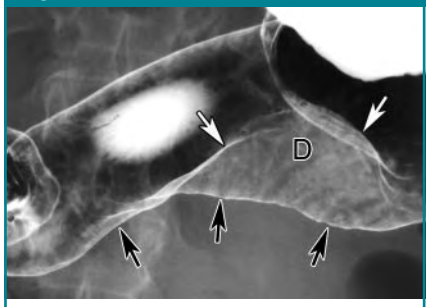

Figure 26: Double-contrast spot image of gastric antrum and body with patient in supine position shows smooth indentation on greater curvature (black arrows) due to extrinsic mass lesion compressing stomach. Second barium-coated line (white arrows) indicates that lumen is narrowed asymmetrically. Area of increased radiopacity *(D)* also results from mass compressing lumen. These findings were caused by massive retroperitoneal lymphoma.

Figure 27

Figure 27: Double-contrast spot image of gastric antrum with patient in supine left posterior oblique position shows ovoid, 1.5-cm smooth-surfaced submucosal lesion (arrows) extending from lesser curvature of distal antrum to adjacent pylorus. This lesion changed in size and shape at fluoroscopy with palpation and peristalsis. Findings are characteristic of hypertrophied antral-pyloric fold.

ume of parietal and chief cell and subsequent hypochlorhydria. The rugal folds may appear massively enlarged and lobulated on barium studies (Fig 29) (91).

Figure 28

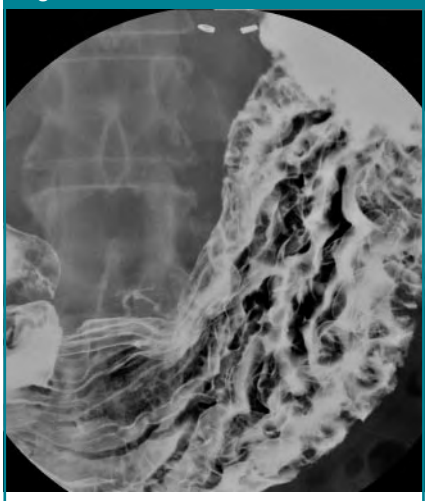

Figure 28: Double-contrast spot image of stomach with patient in supine position shows moderately thickened folds in gastric body due to chronic *Hpylori* gastritis. Folds are considerably less thickened and lobulated than in patient with Menetrier disease (Fig 29). Note surgical clips from prior vagotomy.

Figure 29

Figure 29: Double-contrast spot image of gastric body with patient in supine position shows markedly thickened, lobulated folds and diffuse distortion of areae gastricae pattern in patient with Menetrier disease.

Although early reports stated that fold enlargement predominantly involved the gastric fundus and body (sparing the antrum) (94), later reports found that Menetrier disease causes fold enlargement throughout the stomach in at least 50% of patients (91), presumably because surface foveolar cells line the entire stomach.

Figure 30

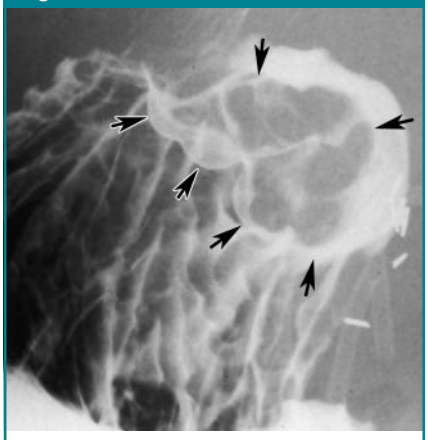

Figure 30: Double-contrast spot image of gastric fundus with patient in right-side-down position shows smooth, undulating submucosal mass (arrows) on posterior wall of fundus extending to cardia. This patient had portal hypertension with a conglomerate mass of gastric varices (also known as tumorous varices). Note surgical clips from recent liver transplantation.

Figure 31

Figure 31: Double-contrast spot image of gastric fundus with patient in right-side-down position shows polypoid mass (arrows) that has obliterated and replaced normal cardiac rosette. Arrowheads denote areas of ulceration within tumor. This patient had an advanced carcinoma of cardia.

Portal hypertension sometimes may cause mucosal hyperemia with dilated submucosal vessels in the absence of true varices, a condition known as portal hypertensive gastropathy (95). This gastropathy can lead to acute or chronic gastrointestinal bleeding. Thickened, finely nodular folds are seen in the gastric fundus on barium studies (96). Gastric varices with associated esophageal varices are usually caused by portal hypertension, whereas isolated gastric varices (in the absence of esophageal varices) may be caused by portal hypertension or, less commonly, by splenic vein obstruction from pancreatic carcinoma, pancreatitis, or pancreatic pseudocysts (97,98). Gastric varices can be distinguished from the abnormal folds of portal hypertensive gastropathy by their undulating and tortuous configuration and smooth contour (Fig 30) (97). In some patients, varices may also be seen on double-contrast studies as multiple smooth, round or ovoid nodules, likened to the appearance of a bunch of grapes. In others, however, a conglomerate mass of gastric varices (also known as tumorous varices) may be manifested as a smooth, undulating submucosal mass on the medial wall of the fundus near the gastric cardia (85).

The normal gastric cardia is usually manifested on double-contrast studies as a stellate collection of thin, smooth folds radiating to a central point at the gastroesophageal junction (Fig 2). Any lesion disrupting or obliterating the cardiac rosette with associated nodularity, mass effect, ulceration, or distorted folds in this region should be considered suspicious for carcinoma of the cardia (Fig 31). More advanced tumors at the cardia may appear as polypoid, ulcerated, or infiltrating lesions that can easily be visualized with a double-contrast technique (Fig 31) (99–101).

Gastric Narrowing

Narrowing of the luminal contour of the stomach may be caused by scarring, infiltrating tumor, or extrinsic diseases secondarily affecting the stomach. Chronic

scarring from peptic ulcer disease may produce asymmetric inbowing and retraction of one wall of the stomach, often associated with smooth, straight folds that radiate to the site of the healed ulcer. Other patients with peptic scarring have smooth, tapered narrowing of the gastric antrum or, less commonly, weblike antral narrowing (Fig 32). Scarring from ingestion of NSAIDs (ie, chronic NSAID gastropathy) can also result in the characteristic flattening of the greater curvature of the distal antrum (102).

Long-segment narrowing of the stomach (either circumferential or confined to one wall) or diffuse narrowing of the stomach is usually caused by an infiltrating or scirrhous gastric carcinoma (103) or metastatic breast cancer. The narrowing with scirrhous carcinoma results from a desmoplastic reaction to tumor cells infiltrating the submucosa, producing a linitis plastica appearance. Scirrhous carcinomas may be manifested as diffuse, long-segment, or even short-segment narrowing of any portion of the stomach (Fig 33) (103). The narrowed lumen is rigid and nondistensible at fluoroscopy, and gastric peristalsis is obliterated in this region. The luminal contour may have a smooth, nodular, or finely ulcerated surface on double-contrast studies (Fig 33). Occasionally, scirrhous carcinomas of the distal antrum may be very short, circumferential lesions confined to the prepyloric region of the stomach (104). It is important to recognize that endoscopy and biopsy have a poor sensitivity in depicting scirrhous carcinomas of the stomach, so that some patients with radiographically diagnosed lesions may require one or more repeat endoscopic examinations to confirm the diagnosis.

In contrast, the narrowing with metastatic breast cancer results from dense infiltration of the submucosa by tumor. Severe scarring from previous caustic ingestion may cause diffuse antral narrowing indistinguishable from antral carcinoma on barium studies, but the clinical history should suggest the correct diagnosis. Tapered narrowing of the gastric antrum may also be caused by antral scarring from Crohn disease or, rarely, other granulomatous diseases such as sarcoidosis, syphilis, and tuberculosis. Occasionally, antral narrowing may also result from gastric atrophy related to the presence of a long-standing gastrojejunal anastomosis without an antrectomy.

Atrophic gastritis is a condition in which body-type mucosal glands are replaced by metaplastic cells resembling pyloric- or intestinal-type epithelium (10). Most atrophic gastritis is related to chronic inflammation rather than autoimmune phenomena. This form of atrophic gastritis is often patchy and macroscopically flat, so that it is not recognizable on barium studies. In other patients with the autoimmune form of atrophic gastritis, there is severe loss of parietal cell mass, resulting in inadequate secretion of intrinsic factor with the subsequent development of vitamin B12 deficiency and, eventually, pernicious anemia. In the later stages of autoimmune atrophic gastritis, decreased parietal cell mass is manifested as a diminished mucosal surface volume and loss of gastric folds. More than 80% of patients with pernicious anemia have a diffusely narrowed stomach with a smooth contour and decreased or absent rugal folds on double-contrast studies (Fig 34).

Figure 32

Figure 32: Double-contrast spot image of distal gastric antrum and duodenal bulb with patient in left posterior oblique position shows short segment of smooth, circumferential narrowing (arrow) due to antral web related to scarring from previous peptic ulcer disease. If mucosal nodularity or irregularity of luminal contour had been present, endoscopy and biopsy would have been required to rule out focal gastric cancer.

Figure 33

Figure 33: Double-contrast spot image of gastric antrum and body with patient in supine position shows long segment of circumferential narrowing extending from mid gastric body to mid gastric antrum (arrows denote limits of tumor). Although tumor surface is predominantly smooth, focal areas of mucosal nodularity are seen in proximal end of lesion (arrowheads). This patient had scirrhous gastric carcinoma producing a linitis plastica appearance.

Figure 34

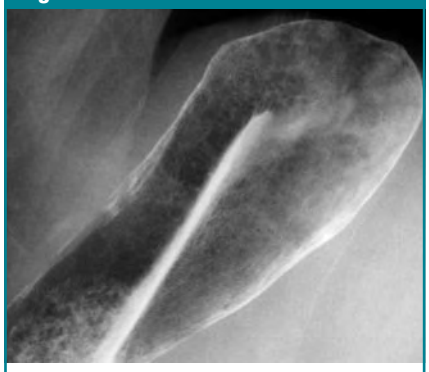

Figure 34: Double-contrast spot image of gastric fundus and body with patient in right-side-down position shows smooth narrowing of fundus and body of stomach with absent rugal folds and small, barely visible areae gastricae. These findings are characteristic of atrophic gastritis.

References

1. Freeny PC. Double-contrast gastrography of the fundus and cardia: normal landmarks and their pathologic changes. AJR Am J Roentgenol 1979;133:481–487.
2. Herlinger H, Grossman R, Laufer I, Kressel HY, Och R. The gastric cardia in double-contrast study: its dynamic image. AJR Am J Roentgenol 1980;135:21–29.
3. Toner PG, Cameron CHS. The gastric mucosa. In: Whitehead R, ed. Gastrointestinal and oesophageal pathology. 2nd ed. Edinburgh, Scotland: Churchill Livingstone, 1995; 15–32.
4. Fenoglio-Preiser CM, Noffsinger AE, Stemmermann GN, Lantz PE, Listrom MB. Gastrointestinal pathology: an atlas and text. Philadelphia, Pa: Lippincott-Raven, 1999; 153–236.
5. Rubesin SE, Furth EE, Levine MS. Gastritis from NSAIDs to Helicobacter pylori. Abdom Imaging 2005;30:142–159.
6. Mackintosh CE, Kreel L. Anatomy and radiology of the areae gastricae. Gut 1977;18:855–864.
7. Seaman WB. The areae gastricae. AJR Am J Roentgenol 1978;131:554.
8. Rubesin SE, Herlinger H. The effect of barium suspension viscosity on the delineation of areae gastricae. AJR Am J Roentgenol 1986;146:35–38.
9. Charagundla SR, Levine MS, Langlotz CP, Rubesin SE, Laufer I. Visualization of areae gastricae on double-contrast gastrointestinal radiography: relationship to age of patients. AJR Am J Roentgenol 2001;177:61–63.
10. Appelman HD. Gastritis: terminology, etiology, and clinicopathologic correlations—another biased view. Hum Pathol 1994;25:1006–1019.
11. Laufer I, Kressel HY. Principles of double-contrast diagnosis. In: Levine MS, Rubesin SE, Laufer I, eds. Double contrast gastrointestinal radiology. 3rd ed. Philadelphia, Pa: Saunders, 2000; 8–46.
12. Laufer I. A simple method for routine double contrast study of the upper gastrointestinal tract. Radiology 1975;117:513–518.
13. Shirakabe H, Kobayashi S, Maruyama M. Principles and application of double contrast radiography. In: Shirakabe H, Nishizawa M, Maruyama S. Atlas of x-ray diagnosis of early gastric cancer. 2nd ed. Tokyo, Japan: Igaku-Shoin, 1982; 19–43.
14. Levine MS, Rubesin SE, Herlinger H, Laufer I. Double contrast upper gastrointestinal examination: technique and interpretation. Radiology 1988;168:593–602.
15. Rubesin SE, Levine MS. Principles for performing a double contrast upper gastrointestinal examination. Westbury, NY: E-Z-EM, 2000; 1–29.
16. Rubesin SE. Gallery of double contrast terminology. Gastroenterol Clin North Am 1995;24:259–288.
17. Cho KC, Gold BM, Printz DA. Multiple transverse folds in the gastric antrum. Radiology 1987;164:339–341.
18. Dheer S, Levine MS, Redfern RO, Metz DC, Rubesin SE, Laufer I. Antral gastritis radiographic findings in patients with and without Helicobacter pylori. Br J Radiol 2002;75:805–811.
19. Levine MS, Palman CL, Rubesin SE, Laufer I, Herlinger H. Atrophic gastritis in pernicious anemia: diagnosis by double contrast radiography. Gastrointest Radiol 1989;14:215–219.
20. Warren JR. Unidentified curved bacilli on gastric epithelium in chronic active gastritis. Lancet 1983;1:1273–1275.
21. Marshall BJ, Warren JR. Unidentified curved bacilli in the stomach of patients with gastritis. Lancet 1984;1:1311–1315.
22. Yardley JH, Hendrix TR. Gastritis, gastropathy, duodenitis, and associated ulcerative lesions. In: Yamada Y, Alpers DH, Laine L, Owyang C, Powell DW, eds. Textbook of gastroenterology. 3rd ed. Philadelphia, Pa: Lippincott Williams & Wilkins, 1999; 1463–1499.
23. Dooley CP, Cohen H, Fitzgibbons PL, et al. Prevalence of Helicobacter pylori infection and histologic gastritis in asymptomatic persons. N Engl J Med 1989;321:1562–1566.
24. Graham DY, Go MF. Helicobacter pylori: current status. Gastroenterology 1993;105:279–282.
25. Bayerdorffer E, Lehn N, Hatz R, et al. Difference in expression of Helicobacter pylori gastritis in antrum and body. Gastroenterology 1992;102:1575–1582.
26. Dixon MF. Helicobacter pylori and peptic ulceration: histologic aspects. J Gastroenterol Hepatol 1991;6:125–130.
27. Parsonnet J, Friedman GD, Vandersteen DP, et al. Helicobacter pylori infection and the risk of gastric carcinoma. N Engl J Med 1991;325:1127–1131.
28. Hansson LE, Engstrand L, Nyren O, et al. Helicobacter pylori infection: independent risk indicator of gastric adenocarcinoma. Gastroenterology 1993;105:1098–1103.
29. Wotherspoon AC, Ortiz-Hidalgo C, Flaxon, Isaccson PG. Helicobacter pylori associated gastritis and primary B-cell gastric lymphoma. Lancet 1991;338:1175–1176.
30. Parsonnet J, Hansen S, Rodriguez L, et al. Helicobacter pylori infection and gastric lymphoma. N Engl J Med 1994;330:1267–1271.
31. Bahk YW, Ahn JR, Choi HJ. Lymphoid hyperplasia of the stomach presenting as umbilicated polypoid lesions. Radiology 1971;100:277–280.
32. Sbeih F, Abdullach A, Sullican S, Merenkow Z. Antral nodularity, gastric lymphoid hyperplasia and Helicobacter pylori in adults. J Clin Gastroenterol 1996;22:227–230.
33. Torigian DA, Levine MS, Gill NS, et al. Lymphoid hyperplasia of the stomach: radiographic findings in five adult patients. AJR Am J Roentgenol 2001;177:71–75.
34. Genta RM, Hamner HW. The significance of lymphoid follicles in the interpretation of gastric biopsy specimens. Arch Pathol Lab Med 1994;118:740–743.
35. Yoo CC, Levine MS, Furth EE, et al. Gastric mucosa-associated lymphoid tissue lymphoma: radiographic findings in six patients. Radiology 1998;208:239–243.
36. Eidt S, Stolte M. Prevalence of lymphoid follicles and aggregates in Helicobacter pylori gastritis in antral and body mucosa. J Clin Pathol 1993;46:832–835.
37. Kaneko E, Nakamura T, Umeda N, Fugino M, Niwa H. Outcome of gastric carcinoma detected by gastric mass survey in Japan. Gut 1977;18:626–630.
38. Kaibara N, Kawaguchi H, Nishidoi H, et al. Significance of mass survey for gastric cancer from the standpoint of surgery. Am J Surg 1981;142:543–545.
39. Montesi A, Graziani L, Pesaresi A, DeNigris E, Bearzi I, Ranaldi R. Radiologic diagnosis of early gastric cancer by routine double-contrast examination. Gastrointest Radiol 1982;7:205–215.
40. Gold RP, Green PH, O'Toole KM, Seaman WB. Early gastric cancer: radiographic experience. Radiology 1984;152:283–290.
41. White RM, Levine MS, Enterline HT, Laufer I. Early gastric cancer: recent experience. Radiology 1985;155:25–27.
42. Shirakabe H, Nishizawa M, Maruyama M, Kobayashi S. Definition and classification of early gastric cancer. In: Shirakabe H, Nishizawa M, Maruyama M, Kobayashi S, eds. Atlas of x-ray diagnosis of early gastric cancer. 2nd ed. Tokyo, Japan: Igaku-Shoin, 1982; 1–18.
43. Laufer I, Hamilton J, Mullens JE. Demon-

stration of superficial gastric erosions by double contrast radiography. Gastroenterology 1975;68:387–391.

44. Op den Orth JO, Dekker W. Gastric erosions: radiological and endoscopic aspects. Radiol Clin (Belg) 1976;45:88–89.
45. Kikuchi Y, Levine MS, Laufer I, Herlinger H. Value of flow technique for double-contrast examination of the stomach. AJR Am J Roentgenol 1986;147:1183–1184.
46. Lanza FL, Nelson RS, Rack MF. A controlled endoscopic study comparing the toxic effects of sulindac, naproxen, aspirin, and placebo on the gastric mucosa of healthy volunteers. J Clin Pharmacol 1984; 24:89–95.
47. Lanza FL. NSAIDS and the gastrointestinal tract. Abdom Imaging 1997;22:1–4.
48. Grace E. Approach to the patient with gross gastrointestinal bleeding. In: Yamada T, ed. Textbook of gastroenterology. Philadelphia, Pa: Lippincott Williams & Wilkins, 2003; 698–723.
49. Levine MS, Verstandig A, Laufer I. Serpiginous gastric erosions caused by aspirin and other nonsteroidal anti-inflammatory drugs. AJR Am J Roentgenol 1986;146:31–34.
50. Roberts DM. Chronic gastritis, alcohol and non-ulcer dyspepsia. Gut 1972;13:768–774.
51. Balthazar EJ, Megibow AJ, Hulnick DH. Cytomegalovirus esophagitis and gastritis in AIDS. AJR Am J Roentgenol 1985;144: 1201–1204.
52. Laufer I, Trueman T. Multiple superficial gastric erosions due to Crohn's disease of the stomach: radiologic and endoscopic diagnosis. Br J Radiol 1976;49:726–728.
53. Ariyama J, Wehlin L, Lindstrom CG, Wenkert A, Roberts GM. Gastroduodenal erosions in Crohn's disease. Gastrointest Radiol 1980;5:121–125.
54. Sloan JM. Acute haemorrahagic gastritis and acute infective gastritis: gastritis caused by physical agents and corrosives—uraemic gastritis. In: Whitehead R, ed. Gastrointestinal and oesophageal pathology. 2nd ed. Edinburgh, Scotland: Churchill-Livingstone, 1995; 461–470.
55. Rumerman J, Rubesin SE, Levine MS, Long WB, Laufer I. Gastric ulceration caused by heater probe coagulation. Gastrointest Radiol 1988;13:200–202.
56. Levine MS, Creteur V, Kressel HY, Laufer I, Herlinger H. Benign gastric ulcers: diagnosis and follow-up with double-contrast radiography. Radiology 1987;164:9–13.
57. Bloom SM, Paul RE JR, Matsue H, Poplack WE, Goldsmith MR. Improved radiographic detection of multiple gastric ulcers. AJR Am J Roentgenol 1977;128:949–952.
58. Braver JM, Paul RE, Philipps E, Bloom S. Roentgen diagnosis of linear ulcers. Radiology 1979;132:29–32.
59. Nelson SW. The discovery of gastric ulcers and the differential diagnosis between benignancy and malignancy. Radiol Clin North Am 1969;7:5–25.
60. Wolf BS. Observations on roentgen features of benign and malignant ulcers. Semin Roentgenol 1971;6:140–150.
61. Ott DJ, Gelfand DW, Wu WC. Detection of gastric ulcer: comparison of single and double-contrast examination. AJR Am J Roentgenol 1982;139:93–97.
62. Barragry TP, Blatchford JW, Allen MO. Giant gastric ulcers: a review of 49 cases. Ann Surg 1986;203:255–259.
63. Kottler RE, Tuft RJ. Benign greater curvature gastric ulcer: the "sump ulcer." Br J Radiol 1981;54:651–654.
64. Hocking BV, Alp MH, Grant AK. Gastric ulceration with hiatus hernia. Med J Aust 1976;2:207–208.
65. Thompson G, Somers S, Stevenson GW. Benign gastric ulcer: a reliable radiologic diagnosis? AJR Am J Roentgenol 1983;141: 331–333.
66. Zboralske FF, Stargardter FL, Harel GS. Profile roentgenographic features of benign greater curvature ulcers. Radiology 1978; 127:63–67.
67. Levine MS, Kelly MR, Laufer I, Rubesin SE, Herlinger H. Gastrocolic fistulas: the increasing role of aspirin. Radiology 1993; 187:359–361.
68. Eisenberg RL, Levine MS. Miscellaneous abnormalities of the stomach. In: Gore RM, Levine MS, eds. Textbook of gastrointestinal radiology. Philadelphia, Pa: Saunders, 2000; 659–681.
69. Treichel J, Gerstenberg E, Palme G, Klemm T. Diagnosis of partial gastric diverticula. Radiology 1976;119:13–18.
70. Gordon R, Laufer I, Kressel HY. Gastric polyps found on routine double-contrast examination of the stomach. Radiology 1980; 134:27–30.
71. Joffe N, Antonioli DA. Atypical appearances of benign hyperplastic polyps. AJR Am J Roentgenol 1978;131:147–152.
72. Smith HJ, Lee EL. Large hyperplastic polyps of the stomach. Gastrointest Radiol 1983;8:19–23.
73. Cherukuri R, Levine MS, Furth EE, Rubesin SE, Laufer I. Giant hyperplastic polyps in the stomach: radiographic findings in seven patients. AJR Am J Roentgenol 2000;175: 1445–1448.
74. Hizawa K, Iida M, Matsumoto T, Aoyagi K, Yao T, Fujisima M. Natural history of fundic gland polyps without familial adenomatous coli: follow-up observations in 31 patients. Radiology 1993;189:429–432.
75. Op den Orth JO, Dekker W. Gastric adenomas. Radiology 1981;141:289–293.
76. Daniel ES, Ludwig SL, Lewin KJ, Ruprecht RM, Rajacich GM, Schwabe AD. The Cronkhite-Canada syndrome: an analysis of clinical and pathologic features and therapy in 55 patients. Medicine 1982;61:293–309.
77. Suster S. Gastrointestinal stromal tumors. Semin Diagn Pathol 1996;13:297–313.
78. Maderal F, Hunter F, Fuselier G, Gonzales-Rogue P, Torres O. Gastric lipomas: an update of clinical presentation, diagnosis and treatment. Am J Gastroenterol 1984; 79:964–967.
79. Megibow AJ, Redmond PE, Bosniak MA, Horowitz L. Diagnosis of gastrointestinal lipomas by CT. AJR Am J Roentgenol 1979; 133:743–745.
80. Imoto T, Nobe T, Koga M, Miyamoto Y, Nakata H. Computed tomography of gastric lipomas. Gastrointest Radiol 1983;8:129–131.
81. Barbosa JJ, Dockerty MB, Waugh JM. Pancreatic heterotopia: a review of the literature and report of 41 authenticated surgical cases of which 25 were clinically significant. Surg Gynecol Obstet 1946;82:527–542.
82. Lai EC, Tompkins RK. Heterotopic pancreas: review of a 26-year experience. Am J Surg 1986;151:697–700.
83. Besemann EF, Auerbach SH, Wolfe WW. The importance of roentgenologic diagnosis of aberrant pancreatic tissue in the gastrointestinal tract. Am J Roentgenol Radium Ther Nucl Med 1969;107:71–76.
84. Rubesin SE, Levine MS, Glick SN. Gastric involvement by omental cakes: radiographic findings. Gastrointest Radiol 1986; 11:223–228.
85. Carucci LR, Levine MS, Rubesin SE, Laufer I. Tumorous gastric varices: radiographic findings in 10 patients. Radiology 1999;212: 861–865.
86. de Lange EE. Radiographic features of gastritis using the biphasic contrast technique. Curr Probl Diagn Radiol 1987;16:273–308.
87. Gelfand DW, Ott DI, Chem MY. Radiologic

evaluation of gastritis and duodenitis. AJR Am J Roentgenol 1999;173:357–361.

88. Sohn J, Levine MS, Furth EE, et al. Helicobacter pylori gastritis: radiographic findings. Radiology 1995;195:763–767.

89. Levine MS, Rubesin SE. The Helicobacter pylori revolution: radiologic perspective. Radiology 1995;195:593–596.

90. Ellison EH, Wilson SD. The Zollinger-Ellison syndrome: re-appraisal and evaluation of 260 registered cases. Ann Surg 1964;160:512–530.

91. Olmsted WW, Cooper PH, Madewell JE. Involvement of the gastric antrum in Menetrier's disease. AJR Am J Roentgenol 1976;126:524–529.

92. Glick SN, Cavanaugh B, Teplick SK. The hypertrophied antral-pyloric fold. AJR Am J Roentgenol 1985;145:547–549.

93. Arora R, Levine MS, Harvey RT, Laufer I, Rubesin SE. Hypertrophied antral-pyloric fold reassessment of radiographic findings in 40 patients. Radiology 1999;213:347–351.

94. Reese DF, Hodgson JR, Dockerty MB. Giant hypertrophy of the gastric mucosa (Menetrier's disease): a correlation of the roentgenographic, pathologic, and clinical findings. Am J Roentgenol Radium Ther Nucl Med 1962;88:619–626.

95. Smart HL, Triger DR. Clinical features, pathophysiology, and relevance of portal hypertensive gastropathy. Endoscopy 1991;23:224–228.

96. Chang D, Levine MS, Ginsberg GG, Rubesin SE, Laufer I. Portal hypertensive gastropathy: radiographic findings in eight patients. AJR Am J Roentgenol 2000;175:1609–1612.

97. Levine MS, Kieu K, Rubesin SE, Herlinger H, Laufer I. Isolated gastric varices: splenic vein obstruction or portal hypertension? Gastrointest Radiol 1990;15:188–192.

98. Muhletaler C. Gerlock J, Goncharenko V, Avant GR, Flexner JM. Gastric varices secondary to splenic vein occlusion: radiographic diagnosis and clinical significance. Radiology 1979;132:593–598.

99. Balthazar EJ, Goldfine S, Davidian NM. Carcinoma of the esophagogastric junction. Am J Gastroenterol 1980;74:237–243.

100. Freeny PC, Marks WM. Adenocarcinoma of the gastroesophageal junction: barium and CT examination. AJR Am J Roentgenol 1982;138:1077–1084.

101. Levine MS, Laufer I, Thompson JJ. Carcinoma of the gastric cardia in young people. AJR Am J Roentgenol 1983;140:69–72.

102. Laveran-Stieber RL, Laufer I, Levine MS. Greater curvature antral flattening: a radiologic sign of NSAID-related gastropathy. Abdom Imaging 1994;19:295–297.

103. Levine MS, Kong V, Rubesin SE, Laufer I, Herlinger H. Scirrhous carcinoma of the stomach radiographic and endoscopic diagnosis. Radiology 1990;175:151–154.

104. Balthazar EJ, Rosenberg H, Davidian MM. Scirrhous carcinoma of the pyloric channel and distal gastric antrum. AJR Am J Roentgenol 1980;134:669–673.

Radiology 2007

This is your reprint order form or pro forma invoice

(Please keep a copy of this document for your records.)

Reprint order forms and purchase orders or prepayments must be received 72 hours after receipt of form either by mail or by fax at 410-820-9765. It is the policy of Cadmus Reprints to issue one invoice per order. **Please print clearly**.

Author Name _____
Title of Article _____
Issue of Journal_____ Reprint # _____ Publication Date _____
Number of Pages_____ KB # _____ Symbol Radiology
Color in Article? Yes / No (Please Circle)

Please include the journal name and reprint number or manuscript number on your purchase order or other correspondence.

Order and Shipping Information

Reprint Costs (Please see page 2 of 2 for reprint costs/fees.)

_____ Number of reprints ordered $_____
_____ Number of color reprints ordered $_____
_____ Number of covers ordered $_____
Subtotal $_____
Taxes $_____

(*Add appropriate sales tax for Virginia, Maryland, Pennsylvania, and the District of Columbia or Canadian GST to the reprints if your order is to be shipped to these locations*.)

First address included, add $32 for each additional shipping address $_____

TOTAL $_____

Shipping Address (cannot ship to a P.O. Box) Please Print Clearly

Name _____
Institution _____
Street _____
City _____ State _____ Zip _____
Country _____
Quantity_____ Fax _____
Phone: Day _____ Evening _____
E-mail Address _____

Additional Shipping Address* (cannot ship to a P.O. Box)

Name _____
Institution _____
Street _____
City _____ State _____ Zip _____
Country _____
Quantity _____ Fax _____
Phone: Day _____ Evening _____
E-mail Address _____

** Add $32 for each additional shipping address*

Payment and Credit Card Details

Enclosed: Personal Check _____
Credit Card Payment Details _____
Checks must be paid in U.S. dollars and drawn on a U.S. Bank.

Credit Card: __ VISA __ Am. Exp. __ MasterCard
Card Number _____
Expiration Date_____
Signature: _____

Please send your order form and prepayment made payable to:

Cadmus Reprints
P.O. Box 751903
Charlotte, NC 28275-1903

Note: Do not send express packages to this location, PO Box.
FEIN #:541274108

Invoice or Credit Card Information

Invoice Address Please Print Clearly
Please complete Invoice address as it appears on credit card statement

Name _____
Institution _____
Department _____
Street _____
City _____ State _____ Zip _____
Country _____
Phone _____ Fax _____
E-mail Address _____

Cadmus will process credit cards and *Cadmus Journal Services* will appear on the credit card statement.

If you don't mail your order form, you may fax it to 410-820-9765 with your credit card information.

Signature _____ Date _____
Signature is required. By signing this form, the author agrees to accept the responsibility for the payment of reprints and/or all charges described in this document.

RB-9/22/06

Radiology 2007

Black and White Reprint Prices

Domestic (USA only)						
# of Pages	50	100	200	300	400	500
1-4	$213	$228	$260	$278	$295	$313
5-8	$338	$373	$420	$453	$495	$530
9-12	$450	$500	$575	$635	$693	$755
13-16	$555	$623	$728	$805	$888	$965
17-20	$673	$753	$883	$990	$1,085	$1,185
21-24	$785	$880	$1,040	$1,165	$1,285	$1,413
25-28	$895	$1,010	$1,208	$1,350	$1,498	$1,638
29-32	$1,008	$1,143	$1,363	$1,525	$1,698	$1,865
Covers	$95	$118	$218	$320	$428	$530

International (includes Canada and Mexico)						
# of Pages	50	100	200	300	400	500
1-4	$263	$275	$330	$385	$430	$485
5-8	$415	$443	$555	$650	$753	$850
9-12	$563	$608	$773	$930	$1,070	$1,228
13-16	$698	$760	$988	$1,185	$1,388	$1,585
17-20	$848	$925	$1,203	$1,463	$1,705	$1,950
21-24	$985	$1,080	$1,420	$1,725	$2,025	$2,325
25-28	$1,135	$1,248	$1,640	$1,990	$2,350	$2,698
29-32	$1,273	$1,403	$1,863	$2,265	$2,673	$3,075
Covers	$148	$168	$308	$463	$615	$768

Minimum order is 50 copies. For orders larger than 500 copies, please consult Cadmus Reprints at 800-407-9190.

Reprint Cover

Cover prices are listed above. The cover will include the publication title, article title, and author name in black.

Shipping

Shipping costs are included in the reprint prices. Domestic orders are shipped via UPS Ground service. Foreign orders are shipped via a proof of delivery air service.

Multiple Shipments

Orders can be shipped to more than one location. Please be aware that it will cost $32 for each additional location.

Delivery

Your order will be shipped within 2 weeks of the journal print date. Allow extra time for delivery.

Color Reprint Prices

Domestic (USA only)						
# of Pages	50	100	200	300	400	500
1-4	$218	$233	$343	$460	$579	$697
5-8	$343	$388	$584	$825	$1,069	$1,311
9-12	$471	$503	$828	$1,196	$1,563	$1,935
13-16	$601	$633	$1,073	$1,562	$2,058	$2,547
17-20	$738	$767	$1,319	$1,940	$2,550	$3,164
21-24	$872	$899	$1,564	$2,308	$3,045	$3,790
25-28	$1,004	$1,035	$1,820	$2,678	$3,545	$4,403
29-32	$1,140	$1,173	$2,063	$3,048	$4,040	$5,028
Covers	$95	$118	$218	$320	$428	$530

International (includes Canada and Mexico))						
# of Pages	50	100	200	300	400	500
1-4	$268	$280	$412	$568	$715	$871
5-8	$419	$457	$720	$1,022	$1,328	$1,633
9-12	$583	$610	$1,025	$1,492	$1,941	$2,407
13-16	$742	$770	$1,333	$1,943	$2,556	$3,167
17-20	$913	$941	$1,641	$2,412	$3,169	$3,929
21-24	$1,072	$1,100	$1,946	$2,867	$3,785	$4,703
25-28	$1,246	$1,274	$2,254	$3,318	$4,398	$5,463
29-32	$1,405	$1,433	$2,561	$3,788	$5,014	$6,237
Covers	$148	$168	$308	$463	$615	$768

Tax Due

Residents of Virginia, Maryland, Pennsylvania, and the District of Columbia are required to add the appropriate sales tax to each reprint order. For orders shipped to Canada, please add 7% Canadian GST unless exemption is claimed.

Ordering

Reprint order forms and purchase order or prepayment is required to process your order. Please reference journal name and reprint number or manuscript number on any correspondence. You may use the reverse side of this form as a proforma invoice. Please return your order form and prepayment to:

Cadmus Reprints
P.O. Box 751903
Charlotte, NC 28275-1903

Note: Do not send express packages to this location, PO Box.
FEIN #:541274108

Please direct all inquiries to:

Rose A. Baynard
800-407-9190 (toll free number)
410-819-3966 (direct number)
410-820-9765 (FAX number)
baynardr@cadmus.com (e-mail)

Reprint Order Forms and purchase order or prepayments must be received 72 hours after receipt of form.